Development 133, 3895-3905 (2006) doi:10.1242/dev.02560

N-cadherin is required for the polarized cell behaviors that drive neurulation in the zebrafish

Elim Hong and Rachel Brewster*

Through the direct analysis of cell behaviors, we address the mechanisms underlying anterior neural tube morphogenesis in the zebrafish and the role of the cell adhesion molecule N-cadherin (N-cad) in this process. We demonstrate that although the mode of neurulation differs at the morphological level between amphibians and teleosts, the underlying cellular mechanisms are conserved. Contrary to previous reports, the zebrafish neural plate is a multi-layered structure, composed of deep and superficial cells that converge medially while undergoing radial intercalation, to form a single cell-layered neural tube. Time-lapse recording of individual cell behaviors reveals that cells are polarized along the mediolateral axis and exhibit protrusive activity. In *N-cad* mutants, both convergence and intercalation are blocked. Moreover, although *N-cad*-depleted cells are not defective in their ability to form protrusions, they are unable to maintain them stably. Taken together, these studies uncover key cellular mechanisms underlying neural tube morphogenesis in teleosts, and reveal a role for cadherins in promoting the polarized cell behaviors that underlie cellular rearrangements and shape the vertebrate embryo.

KEY WORDS: Neural tube, Convergence, Radial intercalation, Protrusive activity, Cell polarity, Adherens junction

INTRODUCTION

Neurulation can be defined as a series of morphogenetic movements that shape the neural tube, the precursor of the brain and spinal cord. Failure to undergo proper neurulation results in severe neural tube birth defects in humans, the most prevalent of which is spina bifida (with a frequency of 1 in 1000 live births) (Copp et al., 2003).

The cellular basis for primary neurulation has been studied extensively in amphibia and amniotes (Colas and Schoenwolf, 2001). In the chick, which has been used as a paradigm for vertebrate neurulation, a broad neural plate bends, forming a groove. The margins of the plate are raised to form neural folds that are brought into apposition at the midline. This process is initiated by regionalized apical constriction of the neural epithelium, resulting in the formation of a medial hinge point and two lateral hinge points. The neural folds are 'passively' displaced medially by forces coming from the non-neural ectoderm, which drive rotation of the neuroepithelium around the lateral hinge points. Once the neural folds have come into close apposition, the epidermis seals over the newly formed neural tube and neural crest cells begin to migrate.

Neurulation in the zebrafish appears different from neurulation in amphibians and amniotes, in part because a neural groove and neural folds are not formed. Rather, the apical surfaces of both flanks of the neural plate become juxtaposed at the midline of the neural keel. A lumen is formed secondarily by cavitation (Schmitz et al., 1993). At a cellular level, neurulation in the zebrafish has been best characterized in the trunk region. The neural tube is thought to originate from a single cell-layered columnar neuroepithelium (Papan and Campos-Ortega, 1994). Neural plate cells at this stage of development are not connected by junctional complexes, suggesting that they may not be fully epithelial (Geldmacher-Voss et al., 2003). However, despite the lack of a clear epithelial cytoarchitecture, several observations suggest that the neural keel is formed by infolding of the neural plate as an organized cell layer, as in amniotes. Neural plate cells have an elongated, epithelial-like morphology that is maintained throughout neurulation. Moreover, cells retain their relative positions, such that there is a close correlation between their original mediolateral position in the neural plate and their final ventrodorsal position in the neural tube. Finally, cells gradually transition from a vertical position in the neural plate to a horizontal position in the neural rod (Papan and Campos-Ortega, 1994). Because the neural tube forms from a pre-existing epithelial substrate that undergoes a folding process, neurulation in the zebrafish is thought to incorporate elements of 'primary neurulation' observed in other vertebrates (Papan and Campos-Ortega, 1994; Lowery and Sive, 2004).

Cadherins constitute a family of calcium-dependent homophilic cell-adhesion molecules. N-cadherin (N-cad, cad 2) belongs to the subfamily of classical cadherins, characterized by five extracellular cadherin-binding domains and an intracellular region that binds β-catenin (β-cat) (Tepass et al., 2000). Classical cadherins are often, but not always, associated with adherens junctions (AJs). These junctional complexes are thought to maintain both tissue integrity and cell polarity (D'Souza-Schorey, 2005). The specific expression of *N-cad* in the neural plate following neural induction (Hatta and Takeichi, 1986; Detrick et al., 1990; Radice et el., 1997) led to the hypothesis that this adhesion molecule may be specifically required for neural tube morphogenesis. Several studies have provided some degree of support to this hypothesis. Misexpression of *N-cad* in the non-neural ectoderm in *Xenopus* affects neural tube size and organization, suggesting that *N-cad* defines the tissue undergoing neurulation (Detrieck et al., 1990; Fujimori et al., 1990). Furthermore, experiments in the chick, using function-blocking antibodies against N-cad or expression of a dominant-negative *N-cad*, highlight a role for N-cad in the maintenance of epithelial integrity, neurulation and neural crest cell migration (Bronner-Fraser et al., 1992; Nakagawa and Takeichi, 1997; Ganzler-Odenthal and Redies, 1998). However, knocking out *N-cad* in the mouse results in a surprisingly subtle neurulation defect, in which a neural tube still forms but has an abnormal, undulated appearance (Radice et al., 1997). This relatively weak phenotype might indicate functional

Department of Biological Sciences, University of Maryland Baltimore County, Baltimore, MD 21250, USA.

*Author for correspondence (e-mail: brewster@umbc.edu)

Accepted 2 August 2006

redundancy with other cadherins. Taken together, these data are consistent with a role for *N-cad* in the maintenance of the neuroepithelium and in neurulation, although the exact role of *N-cad* in neurulation remains unclear.

In contrast to the mouse knock-out phenotype, loss of zebrafish *N-cad* function results in blockage of neural tube formation in the midbrain-hindbrain region and several other neural defects (Lele et al., 2002). *N-cad* mutants have a characteristic 'T-shaped' neural tube, which is thought to result from the failure of lateral, but not medial, cells to converge towards the midline. In order to more directly demonstrate the medial convergence defect, Lele et al. (Lele et al., 2002) transplanted *N-cad* mutant cells to the medial region of the neural plate (future ventral neural tube) of wild-type host embryos. At later stages, these cells relocated to the dorsal region of the host neural tube, which is consistent with impaired convergence. However, given that wild-type and mutant cells are unable to mix (Lele et al., 2002), the above assay may in fact reveal the ability of *N-cad*-positive and *N-cad*-negative cells to sort away from one another (Friedlander et al., 1989).

We re-investigate here mechanisms of neural tube morphogenesis in the zebrafish, focusing on anterior regions, as these are most severely affected in *N-cad* mutants, and address the role of *N-cad* in this process. We demonstrate that the cellular basis for neural tube formation in the zebrafish closely resembles mechanisms used during amphibian neurulation. The zebrafish neural plate is a multi-layered structure, composed of deep and superficial cells that converge medially while undergoing radial intercalation, to form a single cell-layered neural tube. In vivo imaging of individual cell behaviors reveals that cells are polarized along the mediolateral axis and exhibit protrusive activity. In *N-cad* mutants, both convergence and intercalation are blocked. Moreover, although mutant cells are not defective in their ability to form protrusions, they are unable to maintain them stably. These findings thus uncover key cellular mechanisms underlying neural tube morphogenesis in teleosts and directly implicate *N-cad* in the polarized cell movements that may drive this process. The expression of *N-cad* in the neural primordium of all vertebrates following neural induction, and the similarity between mechanisms of neural tube morphogenesis in amphibians and teleosts, suggests a conservation of both cellular and molecular mechanisms.

MATERIALS AND METHODS

Zebrafish strains

All wild-type analyses were performed using the Tubingen Long Fin (TL) strain. The *N-cad* mutant allele *N-cad*^{p79emcf} [a missense mutation in the fifth extracellular domain (Birely et al., 2005)] was obtained from M. Granato (University of Pennsylvania).

DNA and morpholino injections

Plasmids encoding membrane-targeted enhanced Green Fluorescent Protein (mGFP) (R. Harland, University of California, Berkeley) and Xenopus β-catenin-GFP constructs (R. Moon, University of Washington) were prepared using a Qiagen Maxi Prep Kit. Plasmid DNA (200 pg) was injected into one- to four-cell stage embryos. N-cad translation-blocking morpholino (Lele et al., 2002) was obtained from Gene Tools and injected into one- to two-cell stage embryos (10 ng per embryo). Microinjection was performed using a PCI 100 Microinjector (Harvard Apparatus).

Embryo staging

Embryos were collected at stages ranging from tailbud to 24 hpf (Kimmel et al., 1995). Developmental stages in the head region are as follows: neural plate/early neural keel, tailbud-1 somite (som); neural keel, 2-3 som; early neural rod (prior to the formation of AJs), 4-5 som; neural rod, 9-10 som; late neural rod (following the formation of AJs), 12-13 som; and cavitation, 20 som. However, DNA injection transiently retarded neural development, such that injected embryos that exhibited the same number of somites as uninjected controls were often less advanced in terms of neural tube morphogenesis. To avoid confusion, the developmental stage, based on the progression of neurulation, is given together with the somitic stage for all injected specimens for which there is a discrepancy.

Embryo sectioning

Embryos were fixed in 4% paraformaldehyde at 4°C overnight, mounted in 4% low-melting point agarose (Shelton Scientific, IBI) and sectioned at 50 μm intervals using a vibratome (1500 Sectioning System, Vibratome). Sections through the midbrain-hindbrain region were identified based on several criteria: the stage of neurulation, the presence and size of the notochord (beginning at 4-5 som) and otic vesicles (9-10 som onwards), and the thickness of the underlying mesoderm.

Labeling and imaging of fixed preparations

Immunohistochemistry on floating sections was carried out according to Westerfield (Westerfield, 2000). The following antibodies were used: mouse-anti-β-cat (BD Biosciences) at 1:200; rabbit-α-aPKCζ (C-20; Santa Cruz Biotechnology) at 1:200; rabbit-α-phospho Histone3 (Upstate Biotechnology) at 1:200; mouse α-ZO-1 (Zymed laboratories) at 1:200; rabbit-α-Sox3C (a gift from M. Klymkowsky, University of Colorado) at 1:2000. Secondary antibodies conjugated to Alexa-488 or Cy3 (Molecular Probes) were used at 1:200. Alexa-488-phalloidin (Molecular Probes) was used at 1:75. DAPI (Molecular Probes) was used according to the manufacturer's instructions. The sections were imaged with a Zeiss 510 META confocal microscope. Single cell analysis was performed using the LSM software (Zeiss).

Riboprobes, *n-cad* and *dlx3* (plasmids obtained from I. Dawid, NIH), were synthesized and whole-mount in situ hybridization was carried out as described (Thisse et al., 1993). Embryos were mounted in glycerol and imaged using a Zeiss Axioscope2 microscope.

Time-lapse confocal microscopy

For time-lapse microscopy, embryos were dechorionated at 2 som. 1.2% agarose (Shelton Scientific, IBI) was laid on a glass-bottom culture dish (MatTek) and <1 mm holes were made in the agarose. Embryos were mounted in these holes, oriented with the dorsal head region in contact with the glass. They were imaged using the Zeiss Axiovert 200 with a PerkinElmer UltraView LCI (Live Cell Imaging) System. The images were analyzed and processed using the UltraView software, Image J (NIH) and Adobe PhotoShop.

Transmission electron microscopy

Transmission electron imaging was performed as described by Brosamle and Halpern (Brosamle and Halpern, 2002).

RESULTS

The neural plate is a multi-layered epithelium

In order to determine the cellular basis of neural tube formation in anterior regions, cells were labeled by microinjection of mGFP. Because DNA is mosaically inherited in the zebrafish, it is possible to label single cells using this technique. Contrary to the previous assumption that the neural plate is a monolayered epithelium (Papan and Campos-Ortega, 1994), single cell labeling revealed that it is in fact composed of two cell layers at the onset of neurulation. The superficial layer consists of cuboidal cells, situated directly below the enveloping layer (EVL). Cells in the deep layer are columnar, with one pole directly apposed to the basement membrane and the other in contact with the cuboidal cells in the upper layer (Fig. 1A). In order to determine whether the bilayered configuration of the neural plate is specific to anterior regions, we examined the trunk and observed a similar cellular organization (data not shown).

The multi-layered nature of the neural plate was further confirmed using transmission electron microscopy (TEM) imaging (Fig. 2A). However, there remained the possibility that cells in the

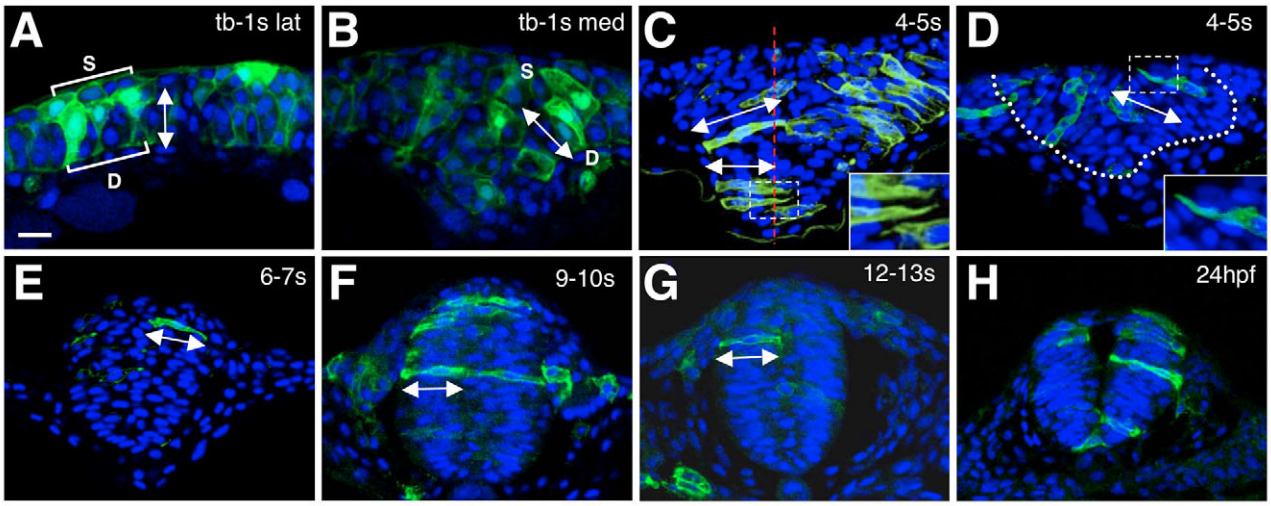

Fig. 1. Analysis of cell behaviors in wild-type embryos. (**A-H**) Cross sections through the anterior neuroepithelium of mGFP (green) and DAPI (blue) labeled embryos. Dorsal is towards the top in all panels; developmental stages are indicated in the upper right corner. C is a composite of multiple focal planes. All other panels are single frames. The insets in C and D are higher magnifications of the boxed in areas. s, superficial cells; d, deep cells; lat, lateral region; med, medial region. Double arrowheads indicate the angular orientation of cells, the dotted red line in C indicates the midline of the neural keel and the dotted white line in D outlines the neural keel. Scale bar: 20 μm.

superficial layer represent a transient population of dividing cells, as mitosis occurs apically in the pseudostratified monolayered epithelium of the chick and mouse neural plate (Sauer, 1935). To address this possibility, we labeled embryos at the neural plate stage with α-phospho Histone3 (α-PH3), a marker for dividing cells, and α-Sox3C, a pan neural marker. We observed that dividing cells are located in both superficial and deep layers of the neural plate, and that nuclei in both layers express Sox3C (Fig. 2B,C), further supporting the multi-layered nature of this tissue.

Radial intercalation resolves the neural epithelium into a single layer

In contrast to the bilayered neural plate, the neuroepithelium of the neural rod and early neural tube is monolayered (Fig. 1E-H). We hypothesized that this transformation occurs via radial intercalation of superficial and deep cells amongst one another. If this hypothesis is correct, the number of cells spanning the entire length of the neuroepithelium should gradually increase as neurulation proceeds, concomitant with a decrease in the number of cells in contact with only one surface. We thus counted the number of labeled cells, following mGFP DNA injection, that were in contact with either the apical, basal or both surfaces of the neuroepithelium at progressive stages of development (see Table S1 in the supplementary material). Cells only in contact with the apical surface (the surface directly below the EVL at the neural plate stage that becomes the midline of the neural tube) represent either superficial cells or cells undergoing mitosis at the neural rod stage (Fig. 1A,B). Cells only in contact with the basal surface (the surface in contact with the basement membrane of the neuroepithelium that becomes the lateral edge of the neural tube) are deep layered cells (Fig. 1A,B), possibly newly differentiated neurons in the neural rod. Cells in contact with both the apical and basal surfaces have undergone radial intercalation and span the full length of the neuroepithelium (Fig. 1E-H). At the neural plate stage, only 5% of cells in lateral regions and 15% of cells in medial regions were in contact with both the apical and basal surfaces. However, these numbers increase dramatically by the late rod stage, as 97% and 72% of cells examined were in contact with both surfaces in dorsal and ventral regions, respectively. These observations suggest that radial intercalation does transform the cellular organization of the neuroepithelium, beginning at the neural plate/early keel stage and extending into the late neural rod stage.

Neuroepithelial cells change orientation and elongate during neurulation

Papan and Campos-Ortega (Papan and Campos-Ortega, 1994) previously reported that neural cells in the trunk region transition from a vertical position in the neural plate to a horizontal position in the neural rod, suggesting that the neural plate infolds as an organized epithelium. A similar process was observed in the head region of embryos injected with mGFP DNA; however, deep and superficial cells initially exhibited distinct behaviors. The angular orientation of cells was measured in degrees ranging from 0° to 90° (see Table S2 in the supplementary material). Values between 0° and 20° correspond to 'horizontal' cells (cells having achieved a close to 90° rotation relative to their initial orientation in the neural plate), values between 60° and 90° to 'vertical' cells (cells that did not significantly change their initial orientation), and values between 20° and 60° to oblique cells. At the neural plate stage, in lateral regions, deep cells were oriented vertically (average angle of 78±6.5°), in contrast to superficial cells that were cuboidal (Fig. 1A). At the same stage, both superficial and deep cells in ventral/medial regions of the neural plate were already inclined towards the midline (average angle of 48±15° and 57±5.8°, respectively; Fig. 1B). At the advanced neural keel stage (4-5 som), cells in lateral regions also adopted an oblique position (average angle of 25±3.1°; Fig. 1C,D), whereas ventral cells became horizontal (average angle of 11±5.4°; Fig. 1C). By the neural rod stage, and continuing into later stages, cells at all dorsoventral levels were fully horizontal (Fig. 1F,G).

Concomitant with the transition to a horizontal position, cells appear to elongate significantly along their future apicobasal axis. At the neural plate stage, the average length-to-width ratio (LWR) of deep lateral cells is 3.5±0.6, whereas, at the advanced neural keel stage (4-5 som), the average LWR of lateral cells is 7.6±0.6 (see

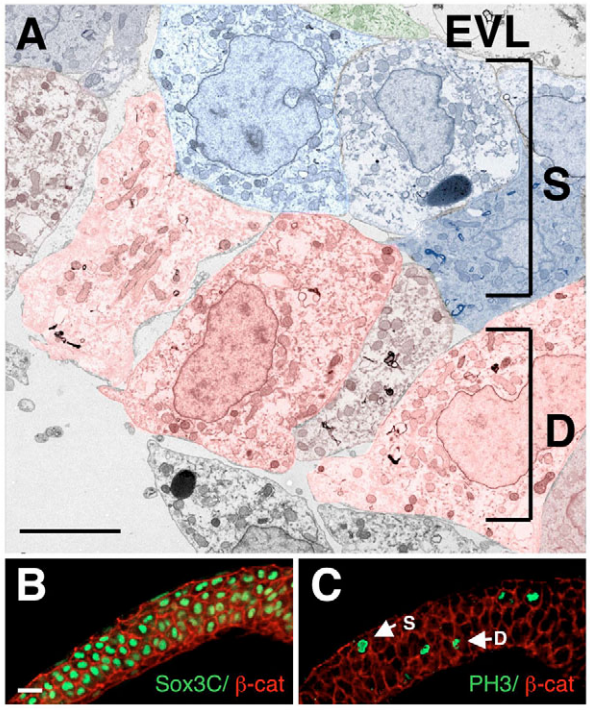

Fig. 2. The neural plate is multi-layered. Cross sections through the anterior lateral neural plate at the tailbud-1 som stage; dorsal is towards the top. (**A**) TEM micrograph, in which superficial cells are pseudocolored in blue, deep cells in red and the EVL in green. (**B**) Embryo double labeled with α-β-cat (red) and α-Sox3C (green). (**C**) Embryo double labeled with α-β-cat (red) and α-PH3 (green). Abbreviations are as in Fig. 1. Scale bars: in A, 5 μm; in B, 20 μm for B,C.

Table S2 in the supplementary material). Thus, neurulation in anterior regions involves cell elongation and a gradual change in angular orientation, which proceeds in a medial to lateral direction, consistent with an infolding mechanism.

Cells exhibit polarized protrusive activity during neurulation

The analysis of single cell behaviors also suggested that cells extend medially directed protrusions (Fig. 1D, inset). This raises the possibility that the infolding process does not occur by passive bending of the neuroepithelium, as in amniotes, but rather by an active medial convergence of cells. To address this possibility, cellular behaviors were imaged from a dorsal view of the neuroepithelium, using time-lapse confocal microscopy. This approach demonstrated that both monopolar and bipolar protrusive activity contribute to neurulation. Cells in the deep cell layer (identified based on their location next to the lateral wall of the neural keel/rod at the beginning of the imaging period) exhibited medially oriented monopolar protrusive activity, while their pole oriented towards the lateral surface of the neural tube remained in contact with the basement membrane (Fig. 3A; see Movie 1 in the supplementary material). By contrast, cells in the superficial layer (that had a medial location at the onset of the imaging period) exhibited bipolar protrusive activity in a mediolateral direction (Fig. 3B). In this cell population, the future apical pole appeared to reach the midline prior to the establishment of basal contact in the majority of cells examined (Fig. 3B; see also Movie 1). Deep and superficial cells elongated considerably as they established contact with both surfaces of the neuroepithelium. It is likely that the protrusive activity exhibited by both cell populations contributes to, and possibly drives, medial convergence and radial intercalation (Brodland, 2006). Because this mode of neurulation does not involve a folding process per se, but rather active en masse cell movement, the term convergence rather than infolding seems more appropriate.

Cells transiently interdigitate at the midline during neural keel formation

As cells from both sides of the neural plate extend medially directed protrusive activity, how do these cellular extensions organize at the midline? Single cell labeling and time-lapse recording revealed that at the neural keel and early neural rod stage, horizontal cells span

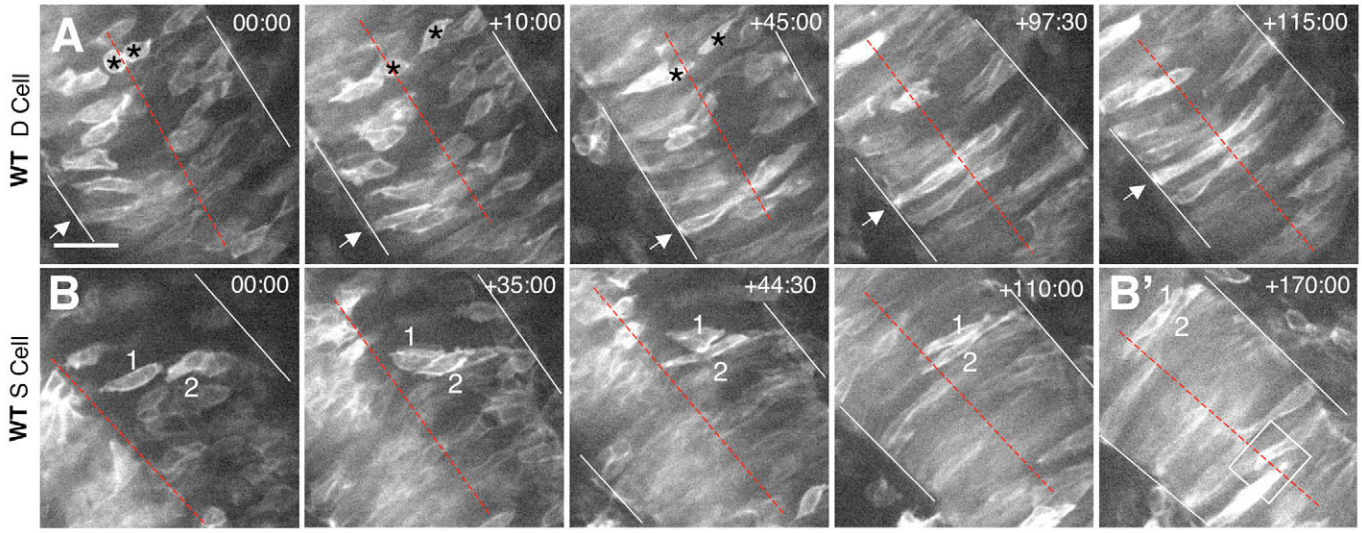

Fig. 3. Time-lapse imaging of wild-type cells. (**A**,**B**) Selected frames from time-lapse confocal movies are shown for a deep (A) and two superficial (B) cells. Time elapsed (in minutes) from the first frame is indicated in the upper right corner. mGFP-labeled embryos were imaged in the hindbrain region, from a dorsal view, beginning at approximately 2-3 som and extending through 6-7 som. Dotted red lines indicate the midline of the neural keel/rod, white lines mark the edges of the neural keel/tube, arrows and numbers indicate individual cells identified in multiple frames, asterisks in A indicate two daughter cells derived from a recent cell division, and the box in B′ shows interdigitation of cells at the midline. Scale bar: 100 μm.

more than the width of the neuroepithelium, suggesting that their extensions cross the midline and interdigitate with those of cells on the opposing side (Fig. 1C, inset; Fig. 3B′). This may account for why the midline is ill defined at the neural keel stage (Fig. 4C). However, interdigitation is transient, as it is no longer observed by the late neural rod stage (Fig. 1G), coincident with the formation of AJs (Fig. 4G).

Loss of *N-cad* causes late but not early neural tube morphogenesis defects

Loss of *N-cad* was previously shown to block neurulation at the neural rod stage (Lele et al., 2002), which is surprisingly late given that *N-cad* is broadly expressed throughout the neuroepithelium following neural induction (Bitzur et al., 1994; Lele et al., 2002). The late onset of neural tube morphogenesis defects was confirmed by labeling *N-cad* mutants at progressive stages of development with *dlx3*, a marker for the edge of the neural plate. Embryos from a cross between two *N-cad*^{p79emcf} heterozygote parents, one quarter of which are expected to be mutant, did not show any difference in the expression of *dlx3* at the neural plate (Fig. 5A) and neural keel (Fig. 5B) stages, suggesting that the convergent extension (CE) movements that shape the neural plate (Keller et al., 1992; Woo and Fraser, 1995) and the early phase of neurulation occur normally in mutants. However, by the neural rod stage, a striking difference in the width of the neural anlage became apparent (wild-type siblings, width of 207±17 nm; *N-cad*^{p79emcf} mutants, width of 309±2 nm; Fig. 5C,D). These observations confirm previous findings and suggest either that *N-cad* is not required for the CE movements that shape the neural plate or that maternal *N-cad* or other cadherins can compensate for loss of *N-cad*.

Other cadherins may compensate for lack of *N-cad* during early stages of neurulation

To further address the requirement for *N-cad* during early stages of neurulation, we analyzed the subcellular distribution of β-cat, a protein associated with the cytoplasmic tail of classical cadherins (Ozawa and Kemler, 1992), in wild type, *N-cad*^{p79emcf} mutants and embryos injected with *N-cad* translation-blocking morpholinos

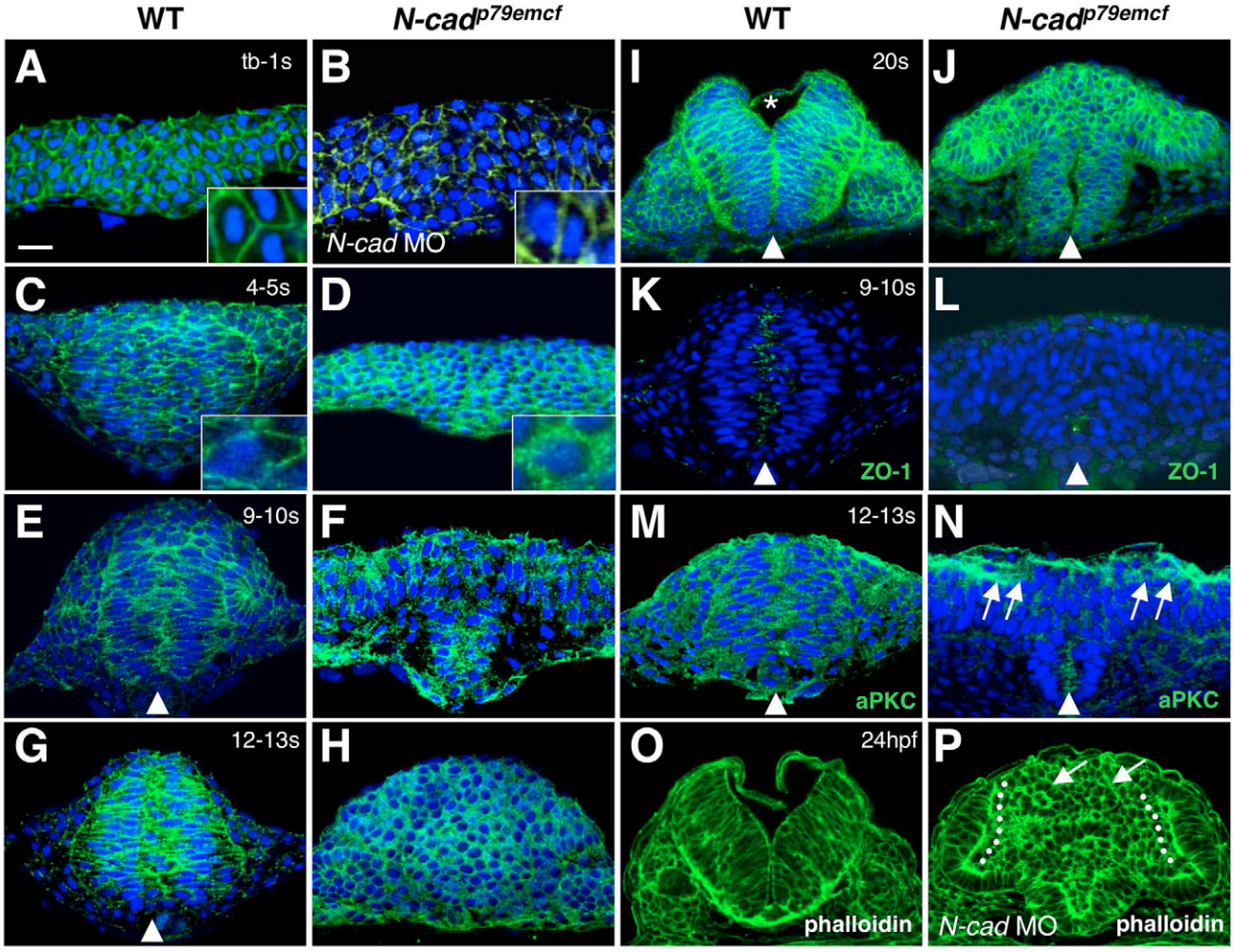

Fig. 4. Analysis of junctional marker expression during neurulation. (**A-P**) Cross sections through the anterior neuroepithelium of wild-type (A,C,E,G,I,K,M,O), *N-cad* MO-injected (B,P) and *N-cad*^{p79emcf} mutant (D,F,H,J,L,N) embryos. Developmental stages are indicated in the upper right corner; dorsal is towards the top in all panels. Embryos were labeled with α-β-cat (A-J), α-ZO-1 (K,L), α-aPKC (M,N), DAPI (A-N) and Alexa-488-phalloidin (O,P). Insets in A-D show higher magnifications of cells. Asterisk in I indicates the position of the forming ventricle, arrowheads point to midline apical labeling, arrows in N point to apical α-aPKC labeling, arrows in P show rosettes, and the dotted line in P indicates apical localization of phalloidin. Scale bar: 20 μm.

(MOs), in which both the maternal and zygotic components should be blocked. At neural plate and early neural rod stages, β-cat is broadly distributed throughout the plasma membrane of wild-type neuroepithelial cells (Fig. 4A,C). β-cat is also observed at normal levels on the cell surface of MO-injected cells at the neural plate stage (Fig. 4B), suggesting that blockage of maternal and zygotic *N-cad* RNA translation is insufficient to disrupt β-cat plasma membrane localization. It is therefore likely that other cadherins function to tether β-cat to the plasma membrane at this stage of development. However, β-cat expression is observed throughout the cytoplasm of *N-cad*^{p79emcf} mutants and is greatly reduced in the plasma membrane of *N-cad* MO-depleted cells at the neural keel and neural rod stages (Fig. 4D; data not shown). The disruption of β-cat localization thus appears to coincide with the onset of neurulation defects observed in mutant and MO-injected embryos, and suggests that *N-cad* is only required during later stages of neural tube morphogenesis. In addition, the defects in β-cat localization suggest that cadherin-based cell-cell adhesion is impaired during neurulation.

Loss of *N-cad* function prevents infolding of lateral neural plate cells

The characteristic 'T-shaped' neural tube of *N-cad* mutants is suggestive of a convergence defect in lateral regions of the neural plate. To investigate the cellular basis of this defect, we analyzed the behavior of single neuroepithelial cells using mGFP. We observed that the cytoarchitecture of the neural plate appears, overall, normal in *N-cad* MO-injected embryos. Cells organize into deep and superficial layers, and deep cells are elongated and in contact with the basement membrane (Fig. 6A). Angular measurements (see Table S2 in the supplementary material) reveal that at early stages of development (tb-1 som), ventral MO-injected cells, surprisingly, are more oblique than their wild-type counterparts (19±5.2° for morphant versus 48±15° for wild type), although LWRs do not increase relative to wild type. At the rod stage, when neurulation in ventral regions is complete in both wild-type and *N-cad*-depleted embryos, the LWR of mutant ventral cells (4.3±0.6) is smaller than that of wild-type ventral cells (6.6±1.4). These findings suggest that, in ventral regions, neurulation is not impaired and may even proceed faster in *N-cad*-depleted embryos, and that cell length has little impact on the initiation or progression of this process.

Additional cellular defects became apparent at the advanced neural keel stage (4-5 som), when a striking difference in the angular orientation of cells was observed in lateral/dorsal regions relative to ventral regions (see Table S2 in the supplementary material). Cells in lateral/dorsal regions of mutant and *N-cad*-depleted embryos, at the neural keel (4-5 som) stage, had a near vertical orientation, with average angles of 65±8.5° and 63±8.8°, respectively (Fig. 6B,C), whereas cells in ventral regions were mostly horizontal, with average angles of 8.4±2.4° and 5.2±1.8°, respectively. By contrast, angles measured for wild-type dorsal neural keel cells were only marginally larger than angles measured for wild-type ventral cells (Table S2 in the supplementary material), indicating that cells along the entire dorsoventral (DV) axis were either oblique or horizontal. Labeling of single cells at later stages revealed that the orientation of lateral/dorsal mutant cells remained close to vertical up until 24 hpf (Fig. 6H). In addition to the cell orientation defects, cell LWRs in lateral/dorsal regions were also abnormal. Although mutant and MO-injected cells retained an epithelial-like morphology, the LWR at the advanced neural keel (4-5 som) and neural rod (6-7 som) stages revealed that *N-cad*-deficient cells failed to elongate as much as wild-type cells in comparable regions. For example, cells in lateral/dorsal regions of wild-type embryos at 4-5 som had an average LWR of 7.6±0.6, relative to 4.4±0.6 and 4.9±0.7 for *N-cad*^{p79emcf} and *N-cad* MO-injected embryos, respectively. Taken together, these observations indicate that, despite the initial accelerated rate of neurulation, loss of N-cad function disrupts the medial convergence and elongation of the neuroepithelium in lateral/dorsal regions.

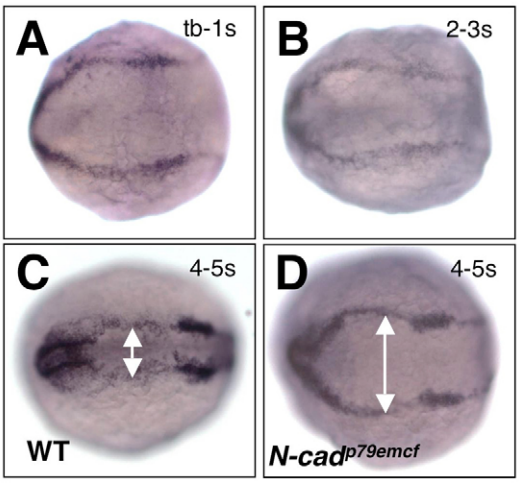

Fig. 5. Neural tube morphogenesis is blocked at the neural keel stage in *N-cad* mutants. (**A-D**) Dorsal view of embryos labeled by in situ hybridization with a *dlx3* riboprobe. Anterior is to the left; developmental stages are indicated in the upper right corner. (A,B) Representative embryos from a cross between two *N-cad*^{p79emcf} heterozygote parents. (C) Wild-type sibling; (D) *N-cad*^{p79emcf} mutant. Double arrowheads indicate the width of the dorsal neural rod.

Loss of *N-cad* function affects radial intercalation in lateral regions

Analysis of single cell behavior in wild-type embryos revealed that medial convergence and radial intercalation occur concomitantly, and both processes are likely to depend on polarized protrusive activity. As loss of *N-cad* function disrupts convergence, we tested whether it also affects radial intercalation (Fig. 6), using the same assay as described previously.

As was observed in wild-type embryos, relatively few mutant and *N-cad*-depleted cells were in contact with both the apical and basal surfaces of the neuroepithelium at the neural plate stage (see Table S1 in the supplementary material). However, numbers were higher for medial *N-cad*-depleted cells (39%) relative to wild-type cells (15%), consistent with the angle measurements, suggesting that neurulation may initially proceed at a faster pace in absence of *N-cad* function.

Numbers of ventral *N-cad*-depleted cells in contact with both the apical and basal surfaces were comparable to wild type at the late neural rod stage: 74% of labeled cells for *N-cad*-depleted embryos relative to 72% of labeled cells for wild type. By contrast, the number of *N-cad*-depleted cells that achieved radial intercalation in dorsal regions (Fig. 6F) did not increase at later stages, relative to wild type. By the late neural rod stage, only 35% of labeled *N-cad*-depleted cells in dorsal regions established apicobasal contact, relative to 97% of labeled wild-type cells in comparable regions. Taken together, these observations suggest that *N-cad* is required for radial intercalation in lateral/dorsal regions. In addition, these results support the idea that radial

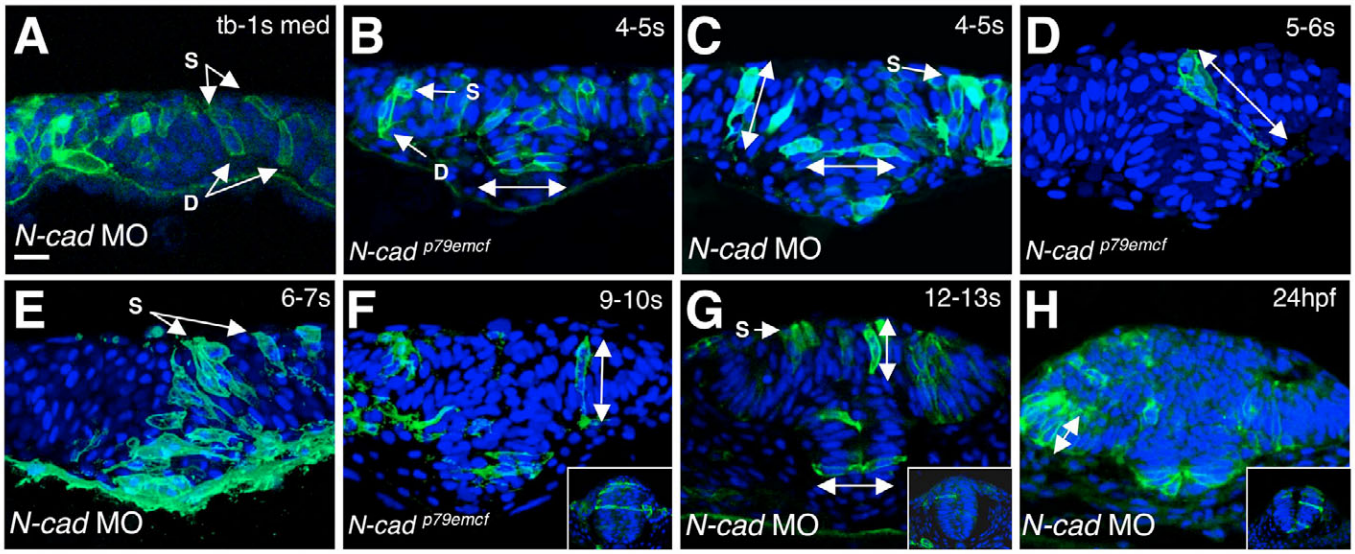

Fig. 6. Analysis of cell behaviors in *N-cad*-depleted embryos. (**A-H**) Cross sections through the anterior neuroepithelium of mGFP and DAPI-labeled MO-injected (A,C,E,G,H) and mutant (B,D,F) embryos. Dorsal is towards the top in all panels; developmental stages are indicated in the upper right corner. C,D and E are composites of multiple focal planes. All other panels are single frames. The insets in F-H are images of wild-type embryos at comparable stages. Abbreviations and symbols are as in Fig. 1. Scale bar: 20 μm.

intercalation and medial convergence are connected, as both occur properly in ventral regions of *N-cad*-deficient embryos and fail to take place in lateral/dorsal regions.

Enhanced cell proliferation has also been reported in the neural tube of *N-cad* mutants at the late neural rod stage (Lele et al., 2002) and may explain the low number of cells in contact with apical and basal surfaces in the neural rod. To investigate whether increased cell division can contribute to the epithelialization defect at earlier stages, wild-type and *N-cad*^{p79emcf} embryos were labeled with the mitotic marker α-PH3. Increased mitosis was not observed at the keel and early neural rod stages (data not shown), when radial intercalation appears defective, and is therefore unlikely to explain the lack of cells with apicobasal contact.

Epithelialization is partially retained in *N-cad* mutants

While impairment of radial intercalation may account for the failure of most lateral/dorsal cells to establish apicobasal contact in the neural rod, this phenotype may be enhanced by the inability of these cells to form junctional complexes at the late neural rod/neural tube stage or to reintegrate into the neuroepithelium upon cell division. Indeed, disruption of *N-cad* function is known to cause a loss of epithelial integrity in both the zebrafish and the chick neural tube, as cells detach from the ventricular walls of the neural tube and populate the ventricles forming cellular aggregates called rosettes (Fig. 4P) (Lele et al., 2002; Ganzler-Odenthal and Redies, 1998).

In order to further address whether the large number of cells that fail to establish apicobasal contact can be partially explained by the inability of cells to form junctional complexes and epithelialize, we analyzed the expression of β-cat, aPKC and ZO-1 (Tjp1 – Zebrafish Information Network). aPKC is a component of the Par3/Par6/aPKC complex that is implicated in the establishment of cell polarity (Izumi et al., 1998; Ohno, 2001) and ZO-1 is a junctional protein associated with both tight junctions and AJs (Itoh et al., 1993). In wild-type embryos at the late neural rod stage, β-cat is distributed throughout the plasma membrane and is increased at the midline of the neural rod, which corresponds to the apical surface of the neuroepithelium where AJs form. Apical localization of β-cat begins in ventral regions (Fig. 4E) and extends dorsally at later stages (Fig. 4G), as has been previously reported (Geldmacher-Voss et al., 2003). During cavitation, wild-type neural progenitor cells appear to be fully polarized, with a clear enrichment of β-cat labeling at the apical surface (Fig. 4I). In *N-cad*^{p79emcf} mutants, β-cat is mislocalized throughout the cytoplasm at the neural rod stage, in both ventral and dorsal regions (Fig. 4D). However, during cavitation, β-cat localization appears enhanced at the apical surface in ventral cells, as observed in wild-type embryos (Fig. 4I,J), suggesting that epithelialization occurs properly, at least in ventral regions. This observation was confirmed by analysis of ZO-1 and aPKC distribution. In wild-type embryos, these junctional proteins become enriched at the midline, prior to β-cat enhancement (Fig. 4E,K; data not shown). Interestingly, in *N-cad*^{p79emcf} mutants, ZO-1 (Fig. 4K,L) and aPKC (Fig. 4M,N) localize to the midline in ventral regions and to the apical surface of the neuroepithelium in lateral/dorsal regions of advanced neural rod stage embryos. Although the apical labeling in lateral/dorsal regions may reflect immunoreactivity of the EVL, neuroepithelial cells located directly below the EVL also appear to be aPKC-positive (Fig. 4N). The ability of at least some lateral/dorsal cells to epithelialize is further evidenced by the apical localization of phalloidin, a marker for polymerized actin, that is closely associated with AJs (Tsukita et al., 1992) in lateral/dorsal regions at 24 hpf (Fig. 4O,P).

These observations suggest that ventral and some lateral/dorsal cells in *N-cad*^{p79emcf} mutants are able to undergo epithelialization. In addition, AJs appear to form downstream of other polarization cues in the neuroepithelium, as aPKC and ZO-1 apical localization precedes that of β-cat, and these markers localize properly in absence of *N-cad*. This hierarchical relationship is also observed in *Drosophila* epithelial cells (Harris and Peifer, 2004).

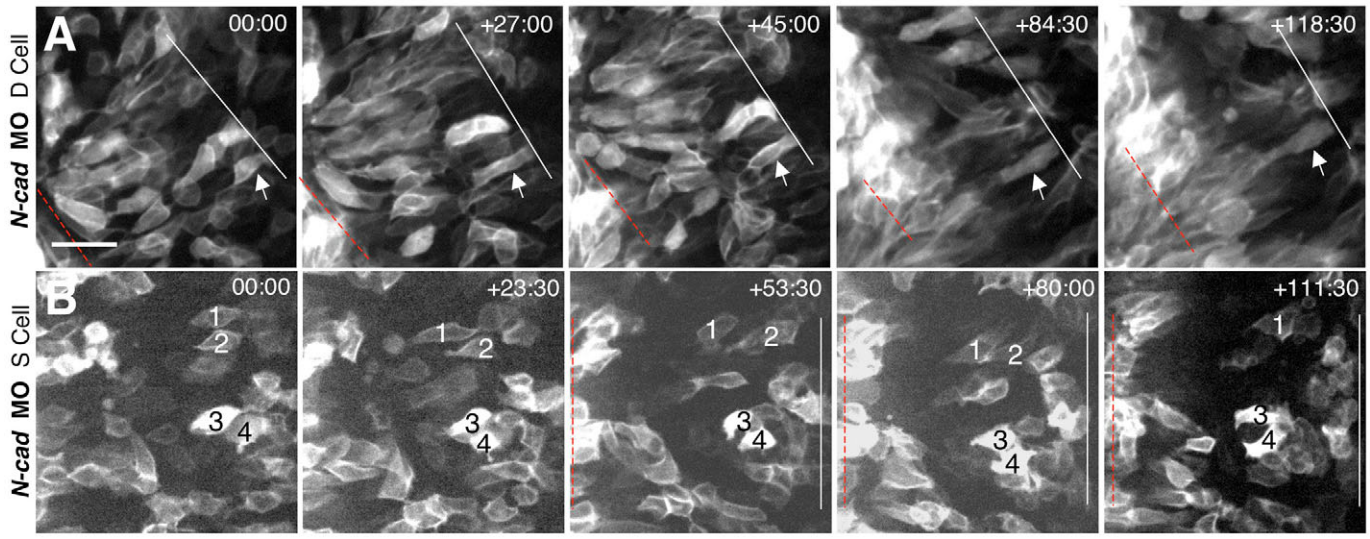

Fig. 7. Time-lapse imaging of *N-cad*-depleted cells. (**A**,**B**) Selected frames from time-lapse confocal movies are shown for deep (A) and superficial (B) cells. Time elapsed (in minutes) from the first frame is indicated in the upper right corner. mGFP-labeled embryos were imaged in the hindbrain region, from a dorsal view, beginning at approximately 2-3 som and extending through 6-7 som. Symbols are as in Fig. 4. Scale bar: 100 μm.

Loss of *N-cad* causes abnormal protrusive activity

What can account for the inability of *N-cad* loss-of-function cells to converge and undergo radial intercalation? Because protrusive activity appears to be involved in both processes in wild-type embryos, we investigated, using time-lapse recording of GFP-labeled cells, whether this activity is impaired by loss of *N-cad* function. Consistent with this hypothesis, deep and superficial cells exhibited protrusive activity oriented along the mediolateral axis; however, they often retracted their cellular extensions (Figs 7, 8; see Movie 2 in the supplementary material). Possibly as a consequence of this abnormal protrusive activity, deep cells did not extend sufficiently to establish contact with the midline (Fig. 7A), and superficial cells failed to migrate medially, elongate and make contact with either the midline or the lateral surfaces of the neuroepithelium (Fig. 7B; see Movie 2 in the supplementary material). The inability of cells to elongate is consistent with the overall decrease in cell length observed in fixed preparations (see Table S2 in the supplementary material). In summary, although cells retain their mediolateral polarity in the absence of *N-cad*, they are unable to form the stable protrusions characteristic of polarized neuroepithelial cells.

One way in which cadherin-based adhesion may function to promote cellular rearrangement is to localize to the poles of cells and mediate the stable anchorage of tractive protrusions (Keller et al., 2000). To address whether cadherin-based adhesion localizes to protrusive ends, we examined the localization of a β-cat-GFP fusion protein in wild-type embryos using time-lapse confocal imaging, following injection of DNA encoding this construct. Interestingly, we observed that β-cat does not appear enhanced at the poles of cells, but rather is evenly distributed throughout the plasma membrane of superficial cells undergoing medial migration (see Movie 3 in the supplementary material). These findings suggest that, if the cadherin-based cell traction model is correct, it is the adhesive activity rather than the adhesive complex itself that becomes localized to sites of protrusive activity.

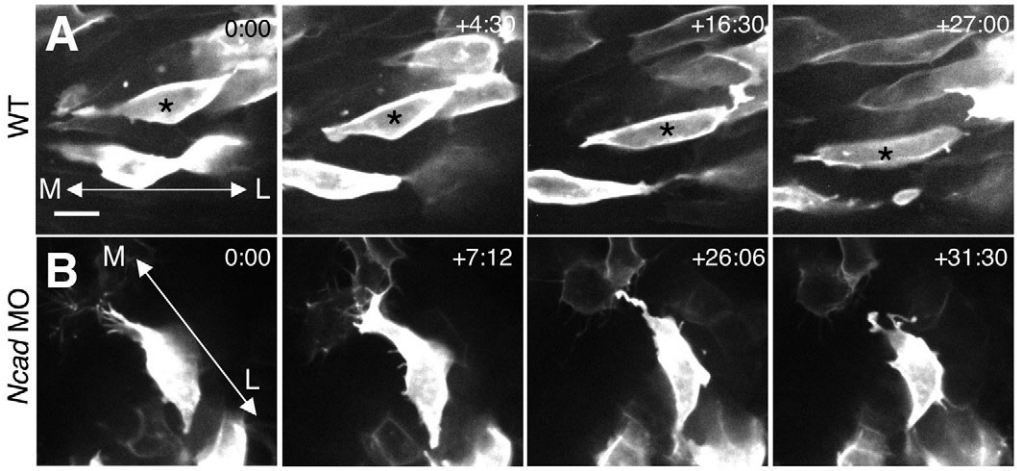

Fig. 8. The protrusive activity in *N-cad*-depleted embryos is unstable. (**A**,**B**) Single frames from time-lapse imaging are shown for wild-type (A) and *N-cad*-depleted (B) superficial cells. Time elapsed (in minutes) from the first frame is indicated in the upper right corner. mGFP-labeled embryos were imaged from a dorsal view, beginning at approximately the 3 som stage and extending through 4-5 som. Asterisks indicate individual cells identified in multiple frames; double arrowheads indicate the orientation of the mediolateral (ML) axis. Scale bar in A: 10 μm.

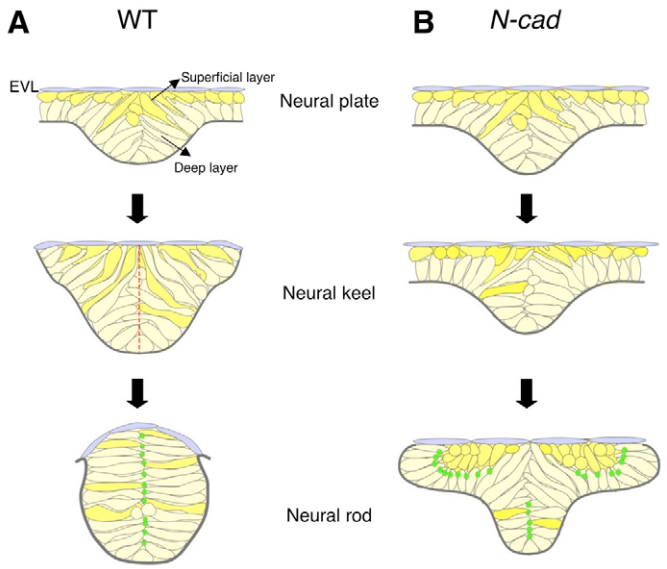

Fig. 9. Model for neurulation in wild-type and *N-cad* embryos. (**A**,**B**) Models for neurulation in wild type (A) and *N-cad* mutants (B). Superficial cells are in dark yellow, deep cells in light yellow and the EVL is in blue. The dotted red line reveals the midline of the neural keel/rod; green dots represent junctional complexes.

DISCUSSION

Model for neurulation in the zebrafish

Based on this study and on previous reports, we propose a model for neurulation in the zebrafish (Fig. 9A). The neural plate starts out as a multi-layered tissue, composed of deep and superficial cells. Deep cells have a columnar, epithelial-like morphology, as they are elongated and maintain contact with the basement membrane. However, neither deep nor superficial cells are strictly epithelial, as they do not have junctional complexes (Gelmacher-Voss et al., 2003) and they are able to cross the midline of the neural keel upon cell division (Kimmel and Warga, 1987; Kimmel et al., 1990; Kimmel et al., 1994; Schmitz et al., 1993; Papan and Campos-Ortega, 1994; Papan and Campos-Ortega, 1997; Papan and Campos-Ortega, 1999; Concha and Adams, 1998; Geldmacher-Voss et al., 2003; Ciruna et al., 2006). During neurulation, cells elongate and converge medially, while simultaneously undergoing radial intercalation. However, deep and superficial cells achieve this by using different mechanisms. Deep cells gradually transition to a horizontal position and insert between superficial cells using medially oriented protrusions. Lateral superficial cells migrate medially, appear to establish contact with the midline first and then the lateral edge of the neural tube, using bipolar mediolaterally oriented protrusive activity. As cells approach the midline they interdigitate transiently with cells in the opposing epithelium, possibly stabilizing the forming neural keel/rod prior to the formation of junctional complexes. Once the neural rod is formed, the neuroepithelium undergoes epithelialization in a ventral to dorsal direction (Gelmacher-Voss et al., 2003; Ciruna et al., 2006), resulting in the loss of midline interdigitations and the establishment of a clear midline. Cavitation of the neural rod follows epithelialization closely and proceeds in the same direction (Schmitz et al., 1993). Elements of this model contributed specifically by this study include: (1) radial intercalation, (2) use of polarized protrusive activity, and (3) transient interdigitation of cells at the midline.

Several key questions remain unanswered regarding neurulation in the zebrafish. In particular, the mechanism enabling cells to initially orient towards the midline in the neural keel is unknown. It is also unclear whether neural crest cells use different mechanisms than the lateral neural plate cells to converge medially.

Role of *N-cad* in mediating cellular rearrangements

By a direct analysis of cellular behaviors, we demonstrate here that, in ventral regions of *N-cad*-depleted embryos, neuroepithelial cells undergo normal, if not accelerated, convergence and intercalation. The accelerated pace of neurulation in ventral regions may be due to a compensatory effect of other genes controlling this process or, possibly, to a non-specific effect of the MO injection. By contrast, cellular rearrangements are greatly impaired in lateral regions (Fig. 9B). These defects are likely to result from the inability of *N-cad*-deficient cells to establish stable protrusive activity, despite proper mediolateral orientation. Because the planar cell polarity (PCP) pathway is also implicated in polarized cell behaviors (Wallingford et al., 2000; Wallingford et al., 2002; Myers et al., 2002; Keller, 2002), it is tempting to speculate that it may regulate or be regulated by the activity of N-cad during neurulation. In support of this idea, the subcellular localization of E-cad, which is required for gastrulation in the zebrafish (Kane et al., 2005; Montero et al., 2005), was recently shown to be regulated by Wnt11, a member of the PCP pathway (Ulrich et al., 2005).

Conservation of mechanisms of neurulation

N-cad is expressed in the neuroepithelium of all vertebrates, at the onset of neural induction. Does this reflect a conservation of cellular and molecular mechanisms of neurulation? At a morphological level, neurulation in teleosts and amphibians appears quite different, given that a neural groove and neural folds form in *Xenopus* but not in the zebrafish. However, there are multiple similarities at the cellular level. The amphibian neural plate is also composed of two layers (Chalmers et al., 2002) that undergo radial intercalation to form a single cell-layered neural tube (Davidson and Keller, 1999). Rather than passively bending towards the midline, prospective dorsal neural cells and neural crest cells migrate using bipolar and monopolar protrusive activity, respectively. Upon completion of neural tube formation, relumination occurs concomitantly with re-epithelialization, in a ventral to dorsal direction (Davidson and Keller, 1999). Thus in both amphibians and teleosts, the neuroepithelium appears more mesenchymal than epithelial, as cellular rearrangement occurs. Despite these similarities, why are neural folds and a neural groove not present in the zebrafish? The formation of both of these structures is dependent upon the ability of cells to undergo regionalized cell shape changes, such as apical or basal constriction (Colas and Schoenwolf, 2001). Apical constriction involves an actomyosin network associated with junctional complexes (Lee and Nagele, 1985; Hildebrand and Soriano, 1999; Haigo et al., 2003; Hildebrand, 2005). However junctional complexes are absent from the zebrafish neuroepithelium prior to neural tube closure. Thus, although amphibian and teleost neuroepithelial cells exhibit many common behaviors, amphibian cells may be ‘more epithelial’ than teleost cells, particularly in the superficial layer, which undergoes apical constriction (Davidson and Keller, 1999). In amniotes, neuroepithelial cells are even more distinctly epithelial, as AJs are present during neurulation (Aaku-Saraste et al., 1996) and cellular rearrangements do not occur during the bending process. It is therefore likely that the architecture of the epithelium imposes physical constraints that dictate the mode of neurulation.

In the zebrafish, *N-cad* is implicated in both the cellular rearrangements that shape the neural tube and the maintenance of neuroepithelial integrity, upon completion of neural tube closure and formation of AJs (Lele et al., 2002) (this study). Thus, *N-cad* appears to play a dual, early and late, role during neural tube development in teleosts. In amphibians, this dual role is likely to be conserved, as cellular mechanisms of neurulation are similar to those in teleosts. However, the epithelial character of the chick neuroepithelium (Aaku-Saraste et al., 1996) suggests that the function of *N-cad* in amniotes may be shifted towards a structural role exclusively, analogous to the late function of *N-cad* in the zebrafish.

In conclusion, our studies reveal a conservation of mechanisms of neurulation in teleosts and amphibians, and highlight an unappreciated role for cadherins in the polarized cell behaviors that shape the vertebrate embryo.

We thank J. Leips, M. Sepanski and P. Jayachandran for assistance with statistical analyses, TEM imaging and in situ hybridization, respectively; M. Granato for the *N-cad*^{p79emcf} allele and M. Klymkowsky for α-Sox3C. In addition, we would like to thank M. Halpern, M. Van Doren, K. Chalasani and M. Harrington for comments on the manuscript. This work was supported by NSF grant 0448432 to R.B. and an NSF ADVANCE, award number SBE-0244880-01.

Supplementary material

Supplementary material for this article is available at http://dev.biologists.org/cgi/content/full/133/19/3895/DC1

References

Aaku-Saraste, E., Hellwig, A. and Huttner, W. B. (1996). Loss of occludin and functional tight junctions, but not ZO-1, during neural tube closure remodeling of the neuroepithelium prior to neurogenesis. *Dev. Biol*. **180**, 664-679.

Birely, J., Schneider, V. A., Santana, E., Dosch, R., Wagner, D. S., Mullins, M. C. and Granato, M. (2005). Genetic screens for genes controlling motor nerve-muscle development and interactions. *Dev. Biol*. **280**, 162-176.

Bitzur, S., Kam, Z. and Geiger, B. (1994). Structure and distribution of N-cadherin in developing zebrafish embryos: morphogenetic effects of ectopic over-expression. *Dev. Dyn*. **201**, 121-136.

Brodland, G. W. (2006). Do lamellipodia have the mechanical capacity to drive convergent extension? *Int. J. Dev. Biol.* **50**, 151-155.

Bronner-Fraser, M., Wolf, J. J. and Murray, B. A. (1992). Effects of antibodies against N-cadherin and N-CAM on the cranial neural crest and neural tube. *Dev. Biol*. **153**, 291-301.

Brosamle, C. and Halpern, M. E. (2002). Characterization of myelination in the developing zebrafish. *Glia* **39**, 47-57.

Chalmers, A. D., Welchman, D. and Papalopulu, N. (2002). Intrinsic differences between the superficial and deep layers of the Xenopus ectoderm control primary neuronal differentiation. *Dev. Cell* **2**, 171-182.

Ciruna, B., Jenny, A., Lee, D., Mlodzik, M. and Schier, A. F. (2006). Planar cell polarity signalling couples cell division and morphogenesis during neurulation. *Nature* **439**, 220-224.

Colas, J. F. and Schoenwolf, G. C. (2001). Towards a cellular and molecular understanding of neurulation. *Dev. Dyn*. **221**, 117-145.

Concha, M. L. and Adams, R. J. (1998). Oriented cell divisions and cellular morphogenesis in the zebrafish gastrula and neurula: a time-lapse analysis. *Development* **125**, 983-994.

Copp, A. J., Greene, N. D. and Murdoch, J. N. (2003). The genetic basis of mammalian neurulation. *Nat. Rev. Genet.* **4**, 784-793.

Davidson, L. A. and Keller, R. E. (1999). Neural tube closure in Xenopus laevis involves medial migration, directed protrusive activity, cell intercalation and convergent extension. *Development* **126**, 4547-4556.

Detrick, R. J., Dickey, D. and Kintner, C. R. (1990). The effects of N-cadherin misexpression on morphogenesis in Xenopus embryos. *Neuron* **4**, 493-506.

D'Souza-Schorey, C. (2005). Disassembling adherens junctions: breaking up is hard to do. *Trends Cell Biol*. **15**, 19-26.

Friedlander, D. R., Mege, R. M., Cunningham, B. A. and Edelman, G. M. (1989). Cell sorting-out is modulated by both the specificity and amount of different cell adhesion molecules (CAMs) expressed on cell surfaces. *Proc. Natl. Acad. Sci. USA* **86**, 7043-7047.

Fujimori, T., Miyatani, S. and Takeichi, M. (1990). Ectopic expression of N-cadherin perturbs histogenesis in Xenopus embryos. *Development* **110**, 97-104.

Ganzler-Odenthal, S. I. and Redies, C. (1998). Blocking N-cadherin function disrupts the epithelial structure of differentiating neural tissue in the embryonic chicken brain. *J. Neurosci.* **18**, 5415-5425.

Geldmacher-Voss, B., Reugels, A. M., Pauls, S. and Campos-Ortega, J. A. (2003). A 90-degree rotation of the mitotic spindle changes the orientation of mitoses of zebrafish neuroepithelial cells. *Development* **130**, 3767-3780.

Haigo, S. L., Hildebrand, J. D., Harland, R. M. and Wallingford, J. B. (2003). Shroom induces apical constriction and is required for hingepoint formation during neural tube closure. *Curr. Biol*. **13**, 2125-2137.

Harris, T. J. and Peifer, M. (2004). Adherens junction-dependent and -independent steps in the establishment of epithelial cell polarity in Drosophila. *J. Cell Biol.* **167**, 135-147.

Hatta, K. and Takeichi, M. (1986). Expression of N-cadherin adhesion molecules associated with early morphogenetic events in chick development. *Nature* **320**, 447-449.

Hildebrand, J. D. (2005). Shroom regulates epithelial cell shape via the apical positioning of an actomyosin network. *J. Cell Sci*. **118**, 5191-5203.

Hildebrand, J. D. and Soriano, P. (1999). Shroom, a PDZ domain-containing actin-binding protein, is required for neural tube morphogenesis in mice. *Cell* **99**, 485-497.

Itoh, M., Nagafuchi, A., Yonemura, S., Kitani-Yasuda, T., Tsukita, S. and Tsukita, S. (1993). The 220-kD protein colocalizing with cadherins in non-epithelial cells is identical to ZO-1, a tight junction-associated protein in epithelial cells: cDNA cloning and immunoelectron microscopy. *J. Cell Biol.* **121**, 491-502.

Izumi, Y., Hirose, T., Tamai, Y., Hirai, S., Nagashima, Y., Fujimoto, T., Tabuse, Y., Kemphues, K. J. and Ohno, S. (1998). An atypical PKC directly associates and colocalizes at the epithelial tight junction with ASIP, a mammalian homologue of Caenorhabditis elegans polarity protein PAR-3. *J. Cell Biol.* **143**, 95-106.

Kane, D. A., McFarland, K. N. and Warga, R. M. (2005). Mutations in half baked/E-cadherin block cell behaviors that are necessary for teleost epiboly. *Development* **132**, 1105-1116.

Keller, R. (2002). Shaping the vertebrate body plan by polarized embryonic cell movements. *Science* **298**, 1950-1954.

Keller, R., Shih, J. and Sater, A. (1992). The cellular basis of the convergence and extension of the Xenopus neural plate. *Dev. Dyn*. **193**, 199-217.

Keller, R., Davidson, L., Edlund, A., Elul, T., Ezin, M., Shook, D. and Skoglund, P. (2000). Mechanisms of convergence and extension by cell intercalation. *Philos. Trans. R. Soc. Lond. B Biol. Sci.* **355**, 897-922.

Kimmel, C. B. and Warga, R. M. (1987). Cell lineages generating axial muscle in the zebrafish embryo. *Nature* **327**, 234-237.

Kimmel, C. B., Warga, R. M. and Schilling, T. F. (1990). Origin and organization of the zebrafish fate map. *Development* **108**, 581-594.

Kimmel, C. B., Warga, R. M. and Kane, D. A. (1994). Cell cycles and clonal strings during formation of the zebrafish central nervous system. *Development* **120**, 265-276.

Kimmel, C. B., Ballard, W. W., Kimmel, S. R., Ullmann, B. and Schilling, T. F. (1995). Stages of embryonic development of the zebrafish. *Dev. Dyn*. **203**, 237-240.

Lee, H. Y. and Nagele, R. G. (1985). Studies on the mechanisms of neurulation in the chick: interrelationship of contractile proteins, microfilaments, and the shape of neuroepithelial cells. *J. Exp. Zool.* **235**, 205-215.

Lele, Z., Folchert, A., Concha, M., Rauch, G. J., Geisler, R., Rosa, F., Wilson, S. W., Hammerschmidt, M. and Bally-Cuif, L. (2002). parachute/n-cadherin is required for morphogenesis and maintained integrity of the zebrafish neural tube. *Development* **129**, 3281-3294.

Lowery, L. A. and Sive, H. (2004). Strategies of vertebrate neurulation and a re-evaluation of teleost neural tube formation. *Mech. Dev*. **121**, 1189-1197.

Montero, J. A., Carvalho, L., Wilsch-Brauninger, M., Kilian, B., Mustafa, C. and Heisenberg, C. P. (2005). Shield formation at the onset of zebrafish gastrulation. *Development* **132**, 1187-1198.

Myers, D. C., Sepich, D. S. and Solnica-Krezel, L. (2002). Convergence and extension in vertebrate gastrulae: cell movements according to or in search of identity? *Trends Genet.* **18**, 447-455.

Nakagawa, S. and Takeichi, M. (1997). N-cadherin is crucial for heart formation in the chick embryo. *Dev. Growth Differ*. **39**, 451-455.

Ohno, S. (2001). Intercellular junctions and cellular polarity: the PAR-aPKC complex, a conserved core cassette playing fundamental roles in cell polarity. *Curr. Opin. Cell Biol*. **13**, 641-648.

Ozawa, M. and Kemler, R. (1992). Molecular organization of the uvomorulin-catenin complex. *J. Cell Biol*. **116**, 989-996.

Papan, C. and Campos-Ortega, J. A. (1994). On the formation of the neural keel and neural tube in the zebrafish Danio (*Brachydanio*) rerio. *Roux's Arch. Dev. Biol.* **203**, 178-186.

Papan, C. and Campos-Ortega, J. A. (1997). A clonal analysis of spinal chord development in the zebrafish. *Dev. Genes Evol.* **207**, 71-81.

Papan, C. and Campos-Ortega, J. A. (1999). Region-specific cell clones in the developing spinal cord of the zebrafish. *Dev. Genes Evol*. **209**, 135-144.

Radice, G. L., Rayburn, H., Matsunami, H., Knudsen, K. A., Takeichi, M. and Hynes, R. O. (1997). Developmental defects in mouse embryos lacking N-cadherin. *Dev. Biol.* **181**, 64-78.

Sauer, F. C. (1935). Mitosis in the neural tube. *J. Comp. Neurol*. **62**, 377-405.

Schmitz, B., Papan, C. and Campos-Ortega, J. A. (1993). Neurulation in the

anterior trunk region of the zebrafish *Bracydanio rerio*. *Roux's Arch. Dev. Biol.* **202**, 250-259.
Tepass, U., Truong, K., Godt, D., Ikura, M. and Peifer, M. (2000). Cadherins in embryonic and neural morphogenesis. *Nat. Rev. Mol. Cell Biol.* **1**, 91-100.
Thisse, C., Thisse, B., Schilling, T. F. and Postlethwait, J. H. (1993). Structure of the zebrafish snail1 gene and its expression in wild-type, spadetail and no tail mutant embryos. *Development* **119**, 1203-1215.
Tsukita, S., Tsukita, S., Nagafuchi, A. and Yonemura, S. (1992). Molecular linkage between cadherins and actin filaments in cell-cell adherens junctions. *Curr. Opin. Cell Biol.* **4**, 834-839.
Ulrich, F., Krieg, M., Schotz, E. M., Link, V., Castanon, I., Schnabel, V., Taubenberger, A., Mueller, D., Puech, P. H. and Heisenberg, C. P. (2005). Wnt11 functions in gastrulation by controlling cell cohesion through Rab5c and E-cadherin. *Dev. Cell* **9**, 555-564.
Wallingford, J. B., Rowning, B. A., Vogeli, K. M., Rothbacher, U., Fraser, S. E. and Harland, R. M. (2000). Dishevelled controls cell polarity during Xenopus gastrulation. *Nature* **405**, 81-85.
Wallingford, J. B., Fraser, S. E. and Harland, R. M. (2002). Convergent extension: the molecular control of polarized cell movement during embryonic development. *Dev. Cell* **2**, 695-706.
Westerfield, M. (2000). *The Zebrafish Book. A Guide for the Laboratory Use of Zebrafish (Danio rerio)* (4th edn). Eugene: University of Oregon Press.
Woo, K. and Fraser, S. E. (1995). Order and coherence in the fate map of the zebrafish nervous system. *Development* **121**, 2595-2609.

Table S1. Percentage of cells undergoing radial intercalation in wild-type, *N-cad*^{p79emcf} mutant and *N-cad* morphant embryos

		Lateral (dorsal) %					Medial %				
		Apical	Basal	Both	Neither	Embryo (cell)	Apical	Basal	Both	Neither	Embryo (cell)
Wild type	Plate (tb-1s)	30	44	5	21	6 (171)	33	42	15	10	6 (110)
	Keel (4-5s)	22	38	14	26	6 (172)	29	35	27	9	6 (101)
	Rod (6-10s)	21	17	62	0	11 (61)	18	5	77	0	11 (60)
	Late rod (12-13s)	3	0	97	0	3 (35)	17	11	72	0	3 (18)
N-cad/MO	Plate (MO; tb-1s)	37	37	4	22	6 (196)	28	33	39*	0	6 (36)
	Keel (*N-cad*; 4-5s)	29	39	11	21	6 (133)	28	15	57§	0	6 (47)
	Keel (MO; 4-5s)	23	27	44	6	5 (100)	40	19	41¶	0	5 (32)
	Rod (*N-cad*; 6-10s)	46	28	24	2	7 (46)	21	4	75	0	7 (67)
	Rod (MO; 6-10s)	48	9	41	2	8 (85)	29	6	64	1	8 (66)
	Late rod (MO; 12-13s)	36	27	35‡	2	4 (45)	22	4	74†	0	4 (51)

Comparisons between the number of cells undergoing intercalation were made using the χ^2-test. (Note: the analysis was performed on cell counts whereas the data shown above are presented as percentages.) Comparisons were statistically significant unless noted otherwise.

*χ_1^2=9.05, P<0.05 when compared with wild-type embryos in the medial region at the neural plate (tb-1s) stage.

$^{\dagger}\chi_1^2$=0.03, P>0.05 (not significant) when compared with wild-type embryos in the medial region at the late rod (12-13s) stage.

$^{\ddagger}\chi_1^2$=31.80, P<0.05 when compared with wild-type embryos in the lateral (dorsal) region at the late rod (12-13s) stage.

$^{\S}\chi_1^2$=13.09, P<0.05 when compared with wild-type embryos in the medial region at the neural keel (4-5s) stage.

$^{\P}\chi_1^2$=2.31, P>0.05 (not significant) when compared with wild-type embryos in the medial region at the neural keel (4-5s) stage.

Table S2. Cell measurements in wild-type, *N-cad*^{p79emcf} mutant and *N-cad* morphant embryos

		Angle (°)			Length (μm)			LWR			
		Ventral	Medial	Lateral/dorsal	Ventral	Medial	Lateral/dorsal	Ventral	Medial	Lateral/dorsal	Embryo (cell)
Wild type	Plate (tb-1s)	48±15	57±5.8	78±6.5	23±3	28±2.7	24±3.8	3.2±0.3	4.2±0.6	3.5±0.6	5 (52)
	Keel (4-5s)	11±5.4	34±6.6	25±3.1*	30±4.7	37±2.9	41±2.7	5±0.8	7±0.7	7.6±0.6†	7 (43)
	Rod (6-7s)	17±3.8	19±5.5	28±3.5	39±6	44±4.5	35±4.2	6.6±1.4	7.6±0.6	6±0.7	4 (30)
N-cad	Plate (tb-1s)	–	–	–	–	–	–	–	–	–	–
	Keel (4-5s)	8.4±2.4	44±12	65±8.5**	29±2.6	35±2.5	34±4	5±1	6.3±1.3	4.4±0.6††	5 (40)
	Rod (6-7s)	18±5.7	45±6.9	67±12.4	24±2.5	36±5.8	32±4.1	4.3±0.6¶	5.2±1.2	4.1±0.9‡‡	4 (27)
MO	Plate (tb-1s)	19±5.2‡	50±7.6	76±4.2	25±2.7	27±2.5	26±2	4.3±0.7§	4±0.6	3.6±0.3	9 (65)
	Keel (4-5s)	5.2±1.8§§	53±6.4	63±8.8**	34±8.1	33±3.6	36±3.5	5.1±1.2	4.8±0.8	4.9±0.7††	4 (77)
	Rod (6-7s)	23±6	43±8.3	69±4.7	25±1.9	38±4.6	33±2.7	4.8±0.4	5.9±0.9	5±0.6	5 (31)

ANOVA was used to analyze the cell measurements. A Tukey post-hoc test was used to distinguish significant pair-wise differences between averages. Comparisons were statistically significant unless noted otherwise. Values are shown as mean±s.e.m.

*$F_{2,40}$=15.39, P<0.05 when comparing cell angle with wild-type embryos in the ventral region ot the neural plate (tb-1s) stage.

$^{\dagger}F_{2,52}$=31.69, P< 0.05 when comparing cell LWR with wild-type embryos in the dorsal region of the neural plate (tb-1s) stage.

$^{\ddagger}F_{1,15}$=11.45, P<0.05 when comparing cell angle with wild-type embryos in the ventral region of the neural plate (tb-1s) stage.

$^{\S}P$>0.05 (not significant) when comparing cell LWR with wild-type embryos in the ventral region of the neural plate (tb-1s) stage.

$^{\P}F_{2,29}$=4.88, P<0.05 when comparing cell LWR with wild-type embryos in the ventral region of the neural rod (6-7s) stage.

**$F_{2,88}$=33.45, P<0.05 when comparing cell angle with wild-type embryos in the dorsal region of the neural keel (4-5s) stage.

$^{\dagger\dagger}F_{2,88}$=17.60, P<0.05 when comparing cell LWR with wild-type embryos in the dorsal region of the neural keel (4-5s) stage.

$^{\ddagger\ddagger}F_{2,25}$=3.29, P<0.05 when comparing cell LWR with wild-type embryos in the dorsal region of the neural rod (6-7s) stage.

$^{\S\S}P$>0.05 (not significant) when comparing cell angle with wild-type embryos in the ventral region of the neural keel (4-5s) stage.